Nonlinear Bloch modes in two-dimensional photonic lattices

Denis Träger[1,2], Robert Fischer[1], Dragomir N. Neshev[1], Andrey A. Sukhorukov[1], Cornelia Denz[2], Wieslaw Królikowski[1], and Yuri S. Kivshar[1]

[1]*Nonlinear Physics Centre and Laser Physics Centre, Centre for Ultrahigh bandwidth Devices for Optical Systems (CUDOS), Research School of Physical Sciences and Engineering, Australian National University, Canberra, ACT 0200, Australia*

[2]*Institut für Angewandte Physik, Westfälische Wilhelms-Universität, 48149 Münster, Germany*

dtraeger@uni-muenster.de

http://www.rsphysse.anu.edu.au/nonlinear

http://www.uni-muenster.de/physik/ap/denz

Abstract: We generate experimentally different types of two-dimensional Bloch waves of a square photonic lattice by employing the phase imprinting technique. We probe the local dispersion of the Bloch modes in the photonic lattice by analyzing the linear diffraction of beams associated with the high-symmetry points of the Brillouin zone, and also distinguish the regimes of normal, anomalous, and anisotropic diffraction through observations of nonlinear self-action effects.

OCIS codes: (190.4420) Nonlinear optics, transverse effects in; (190.5940) Self-action effects; (050.1950) Diffraction gratings.

References and links

1. J. D. Joannopoulos, R. D. Meade, and J. N. Winn, *Photonic Crystals: Molding the Flow of Light* (Princeton University Press, Princeton, 1995).
2. P. S. Russell, "Bloch wave analysis of dispersion and pulse-propagation in pure distributed feedback structures," J. Mod. Opt. **38,** 1599–1619 (1991).
3. P. St. J. Russell, T. A. Birks, and F. D. Lloyd Lucas, "Photonic Bloch waves and photonic band gaps," in *Confined Electrons and Photons*, E. Burstein and C. Weisbuch, eds., (1995), pp. 585–633.
4. H. S. Eisenberg, Y. Silberberg, R. Morandotti, and J. S. Aitchison, "Diffraction management," Phys. Rev. Lett. **85,** 1863–1866 (2000).
5. T. Pertsch, T. Zentgraf, U. Peschel, A. Brauer, and F. Lederer, "Anomalous refraction and diffraction in discrete optical systems," Phys. Rev. Lett. **88,** 093901–4 (2002).
6. M. Lončar, D. Nedeljković, T. P. Pearsall, J. Vučković, A. Scherer, S. Kuchinsky, and D. C. Allan, "Experimental and theoretical confirmation of Bloch-mode light propagation in planar photonic crystal waveguides," Appl. Phys. Lett. **80,** 1689–1691 (2002).
7. P. E. Barclay, K. Srinivasan, M. Borselli, and O. Painter, "Probing the dispersive and spatial properties of photonic crystal waveguides via highly efficient coupling from fiber tapers," Appl. Phys. Lett. **85,** 4–6 (2004).
8. S. I. Bozhevolnyi, V. S. Volkov, T. Sondergaard, A. Boltasseva, P. I. Borel, and M. Kristensen, "Near-field imaging of light propagation in photonic crystal waveguides: explicit role of Bloch harmonics," Phys. Rev. B **66,** 235204–9 (2002).
9. H. Gersen, T. J. Karle, R. J. P. Engelen, W. Bogaerts, J. P. Korterik, N. F. Hulst, van, T. F. Krauss, and L. Kuipers, "Direct observation of Bloch harmonics and negative phase velocity in photonic crystal waveguides," Phys. Rev. Lett. **94,** 123901–4 (2005).

#10229 - $15.00 USD Received 9 January 2006; received 15 February 2006; accepted 17 February 2006

10. R. J. P. Engelen, T. J. Karle, H. Gersen, J. P. Korterik, T. F. Krauss, L. Kuipers, and N. F. Hulst, van, "Local probing of Bloch mode dispersion in a photonic crystal waveguide," Opt. Express **13,** 4457–4464 (2005), http://www.opticsexpress.org/abstract.cfm?URI=OPEX-13-12-4457.
11. Yu. I. Voloshchenko, Yu. N. Ryzhov, and V. E. Sotin, "Stationary waves in non-linear, periodically modulated media with higher group retardation," Zh. Tekh. Fiz. **51,** 902–907 (1981) (in Russian) [English translation: Tech. Phys. **26,** 541–544 (1981)].
12. W. Chen and D. L. Mills, "Gap solitons and the nonlinear optical-response of superlattices," Phys. Rev. Lett. **58,** 160–163 (1987).
13. D. N. Christodoulides and R. I. Joseph, "Discrete self-focusing in nonlinear arrays of coupled wave-guides," Opt. Lett. **13,** 794–796 (1988).
14. C. M. de Sterke and J. E. Sipe, "Gap solitons," in *Progress in Optics*, E. Wolf, ed., (North-Holland, Amsterdam, 1994), Vol. XXXIII, pp. 203–260.
15. J. Feng, "Alternative scheme for studying gap solitons in an infinite periodic Kerr medium," Opt. Lett. **18,** 1302–1304 (1993).
16. R. F. Nabiev, P. Yeh, and D. Botez, "Spatial gap solitons in periodic nonlinear structures," Opt. Lett. **18,** 1612–1614 (1993).
17. S. John and N. Akozbek, "Nonlinear-optical solitary waves in a photonic band-gap," Phys. Rev. Lett. **71,** 1168–1171 (1993).
18. N. Akozbek and S. John, "Optical solitary waves in two- and three-dimensional nonlinear photonic band-gap structures," Phys. Rev. E **57,** 2287–2319 (1998).
19. S. F. Mingaleev and Yu. S. Kivshar, "Self-trapping and stable localized modes in nonlinear photonic crystals," Phys. Rev. Lett. **86,** 5474–5477 (2001).
20. B. J. Eggleton, C. M. de Sterke, and R. E. Slusher, "Nonlinear pulse propagation in Bragg gratings," J. Opt. Soc. Am. B **14,** 2980–2993 (1997).
21. Y. V. Kartashov, V. A. Vysloukh and L. Torner, "Soliton trains in photonic lattices," Opt. Express **12,** 2831 (2004), http://www.opticsexpress.org/abstract.cfm?URI=OPEX-12-13-2831.
22. J. Hudock, N. K. Efremidis and D. N. Christodoulides, "Anisotropic diffraction and elliptic discrete solitons in two-dimensional waveguide arrays," Opt. Lett. **29,** 268–270 (2004).
23. D. Mandelik, H. S. Eisenberg, Y. Silberberg, R. Morandotti, and J. S. Aitchison, "Band-gap structure of waveguide arrays and excitation of Floquet-Bloch solitons," Phys. Rev. Lett. **90,** 053902–4 (2003).
24. A. A. Sukhorukov, D. Neshev, W. Królikowski, and Yu. S. Kivshar, "Nonlinear Bloch-wave interaction and Bragg scattering in optically induced lattices," Phys. Rev. Lett. **92,** 093901–4 (2004).
25. C. M. de Sterke, "Theory of modulational instability in fiber Bragg gratings," J. Opt. Soc. Am. B **15,** 2660–2667 (1998).
26. J. Meier, G. I. Stegeman, D. N. Christodoulides, Y. Silberberg, R. Morandotti, H. Yang, G. Salamo, M. Sorel, and J. S. Aitchison, "Experimental observation of discrete modulational instability," Phys. Rev. Lett. **92,** 163902–4 (2004).
27. R. Iwanow, G. I. Stegeman, R. Schiek, Y. Min, and W. Sohler, "Discrete modulational instability in periodically poled lithium niobate waveguide arrays," Opt. Express **13,** 7794–7799 (2005), http://www.opticsexpress.org/abstract.cfm?URI=OPEX-13-20-7794.
28. M. Stepić, C. Wirth, C. Rüter, and D. Kip, "Experimental observation of modulational instability in self-defocusing nonlinear waveguide arrays," Opt. Lett. **31,** 247–249 (2006).
29. M. Chauvet, G. Fu, G. Salamo, J. W. Fleischer, and M. Segev, "Experimental Observation of Discrete Modulation Instability in 1-D Nonlinear Waveguide Arrays," In *Nonlinear Guided Waves and Their Applications*, Postconference ed. OSA p. WD39 (Optical Society of America, Washington DC, 2005).
30. B. J. Eggleton, C. M. de Sterke, A. B. Aceves, J. E. Sipe, T. A. Strasser, and R. E. Slusher, "Modulational instability and tunable multiple soliton generation in apodized fiber gratings," Opt. Commun. **149,** 267–271 (1998).
31. G. Bartal, O. Cohen, H. Buljan, J. W. Fleischer, O. Manela, and M. Segev, "Brillouin zone spectroscopy of nonlinear photonic lattices," Phys. Rev. Lett. **94,** 163902–4 (2005).
32. N. K. Efremidis, S. Sears, D. N. Christodoulides, J. W. Fleischer, and M. Segev, "Discrete solitons in photorefractive optically induced photonic lattices," Phys. Rev. E **66,** 046602–5 (2002).
33. *Nonlinear Photonic Crystals*, Vol. 10 of *Springer Series in Photonics*, R. E. Slusher and B. J. Eggleton, eds., (Springer-Verlag, Berlin, 2003).
34. J. W. Fleischer, M. Segev, N. K. Efremidis, and D. N. Christodoulides, "Observation of two-dimensional discrete solitons in optically induced nonlinear photonic lattices," Nature **422,** 147–150 (2003).
35. H. Martin, E. D. Eugenieva, Z. G. Chen, and D. N. Christodoulides, "Discrete solitons and soliton-induced dislocations in partially coherent photonic lattices," Phys. Rev. Lett. **92,** 123902–4 (2004).
36. O. Cohen, B. Freedman, J. W. Fleischer, M. Segev, and D. N. Christodoulides, "Grating-mediated waveguiding," Phys. Rev. Lett. **93,** 103902–4 (2004).
37. B. Freedman, O. Cohen, O. Manela, M. Segev, J. W. Fleischer, and D. N. Christodoulides, "Grating-mediated wave guiding and holographic solitons," J. Opt. Soc. Am. B **22,** 1349–1355 (2005).

#10229 - $15.00 USD Received 9 January 2006; received 15 February 2006; accepted 17 February 2006

38. R. Fischer, D. Träger, D. N. Neshev, A. A. Sukhorukov, W. Królikowski, C. Denz, and Yu. S. Kivshar, "Reduced-symmetry two-dimensional solitons in photonic lattices," Phys. Rev. Lett. **96,** 023905–4 (2006).
39. O. Manela, O. Cohen, G. Bartal, J. W. Fleischer, and M. Segev, "Two-dimensional higher-band vortex lattice solitons," Opt. Lett. **29,** 2049–2051 (2004).
40. G. Bartal, O. Manela, O. Cohen, J. W. Fleischer, and M. Segev, "Observation of second-band vortex solitons in 2D photonic lattices," Phys. Rev. Lett. **95,** 053904–4 (2005).

1. Introduction

The study of the wave propagation in optical periodic structures such as photonic crystals [1] has attracted growing interest in recent years. The periodic photonic structures exhibit unique properties allowing to manipulate the flow of light at the wavelength scale and create the basis for novel types of integrated optical devices. In such periodic dielectric structures, the propagation of light is governed by the familiar Bloch theorem due to the interplay between the light and the surrounding periodic structure [2], that introduces the spatially extended linear waves, the so-called Bloch waves, as the eigenmodes of the corresponding periodic potential. Thus, the properties of electromagnetic waves in periodic structures are fully determined by the Bloch wave dispersion which, for the spatial beam propagation, represents the relation between the longitudinal and transverse components of the Bloch wavevector. Since any finite beam can be expressed as a superposition of such Bloch waves [3], the beam propagation in any periodic structure is also determined from the local dispersion. In particular, the beam propagation direction is defined by the normal to the dispersion curve while the beam spreading is governed by the curvature of this curve.

The study of Bloch waves and their temporal and spatial dispersion provides a key information about overall properties of any periodic structure. In particular, depending on the local dispersion and a local value of the wave vector, an optical beam (or pulse) experience normal, anomalous or even vanishing diffraction (or dispersion) [3, 4, 5]. Experimentally, the Bloch-wave character of electromagnetic waves in photonic crystal waveguides has been deduced indirectly by detecting the out-of-plane leakage of light [6], by investigating the evanescent field coupling between a tapered optical fiber and a photonic crystal waveguide [7], and more directly by local near-field probing of the intensity distribution in a waveguide [8]. The full band structure of a photonic crystal waveguide has been recovered very recently by employing a near-field optical microscope and probing both the local phase and amplitude of the light propagating through a single-line defect waveguide [9, 10].

The Bloch-wave dynamics in periodic structures becomes even more dramatic in the presence of the nonlinear medium response that may lead to the formation of strongly localized structures, discrete and gap solitons [11, 12, 13, 14, 15, 16, 17, 18, 19, 20, 21, 22]. The properties of the Bloch modes of nonlinear periodic structures have been extensively studied in the one-dimensional geometries, including the Bragg gratings and waveguide arrays [23, 24], as well as the study of modulational instability of one-dimensional waves [25, 26, 27, 28, 29, 30]. More recently, the Brillouin zone structure of nonlinear two-dimensional photonic lattices was characterized based on the features of collective wave dynamics for partially coherent multi-band excitations [31]. Nevertheless, to the best of our knowledge, no experimental studies of individual two-dimensional Bloch waves from different bands and probing the Bloch wave local dispersion have been reported yet.

The aim of this paper is twofold. First, we probe the local spatial dispersion of the Bloch modes of a two-dimensional optically-induced photonic lattice by analyzing the evolution of linear and nonlinear propagation modes associated with the high-symmetry points of the first Brillouin zone. In particular, we excite the Bloch waves associated with the high-symmetry points of the two-dimensional lattice by matching their unique phase structure and observe different regimes of the linear diffraction. Second, we employ a strong self-focusing nonlinearity

#10229 - $15.00 USD Received 9 January 2006; received 15 February 2006; accepted 17 February 2006

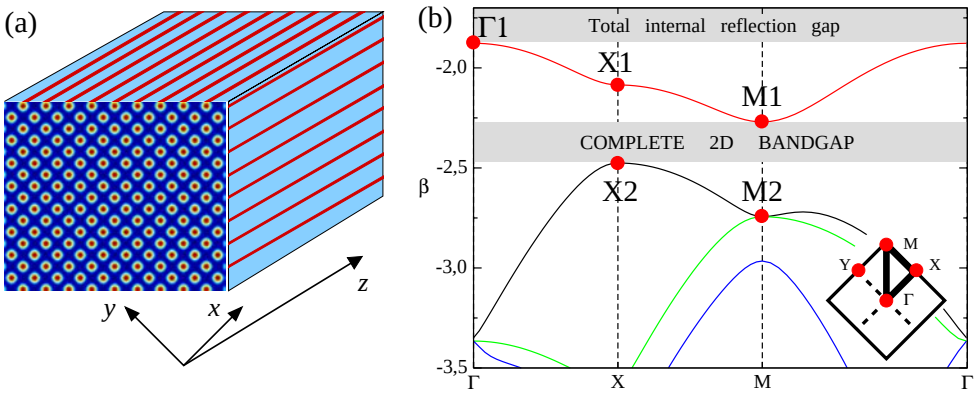

Fig. 1. (a) Experimental image of a two-dimensional optically-induced photonic lattice, that is spatially periodic in the transverse directions (x,y) and stationary along the longitudinal direction z. (b) Calculated bandgap dispersion $\beta(K)$. Dots indicate the main symmetry points. Inset in (b) depicts the corresponding first Brillouin zone.

and study nonlinear self-action effects for the two-dimensional Bloch waves. This allows us to probe and characterize the spatial diffraction of each particular Bloch mode, depending on the curvature of the dispersion surfaces at the corresponding point of the Brillouin zone.

2. Two-dimensional Bloch waves: theoretical background

We study the propagation of an extraordinary polarized optical beam (a probe beam) in a biased photorefractive crystal with an optically induced two-dimensional photonic lattice. We consider a spatially periodic pattern of the refractive index in the form of a square lattice, which is stationary in the longitudinal (z) direction [Fig. 1(a)]. The photonic lattice is formed by the interference of four mutually coherent ordinary polarized optical beams. This interference pattern [Fig. 1(a)],

$$I_p(x,y) = I_g\{\cos[\pi(x+y)/d] + \cos[\pi(x-y)/d]\}^2,$$

induces a refractive index modulation of the crystal for extraordinary polarized light via the strong electro-optic effect [32]. Here x and y are the transverse coordinates, and d is the lattice period. The spatial evolution of the extraordinary polarized beam with a slowly varying amplitude $E(x,y,z)$ propagating along the lattice is then governed by the following nonlinear parabolic equation,

$$i\frac{\partial E}{\partial z} + D\left(\frac{\partial^2 E}{\partial x^2} + \frac{\partial^2 E}{\partial y^2}\right) + \mathscr{F}(x,y,|E|^2)E = 0, \tag{1}$$

where

$$\mathscr{F}(x,y,|E|^2) = -\frac{\gamma}{I_b + I_p(x,y) + |E|^2} \tag{2}$$

describes the refractive index change that includes the two-dimensional lattice itself and the self-induced index change from the probe beam. The parameters used for numerical calculations are chosen to match the conditions of typical experiments discussed below: the dimensionless variables x, y, z are normalized to the typical scale $x_s = y_s = 1$ μm, and $z_s = 1$ mm, respectively; the diffraction coefficient is $D = z_s\lambda/(4\pi n_0 x_s^2)$; $n_0 = 2.35$ is the refractive index of a bulk photorefractive crystal, $\lambda = 532$ nm is the laser wavelength in vacuum, the parameter $I_b = 1$ is the constant dark irradiance, $\gamma = 2.36$ is a nonlinear coefficient proportional to the

#10229 - $15.00 USD Received 9 January 2006; received 15 February 2006; accepted 17 February 2006

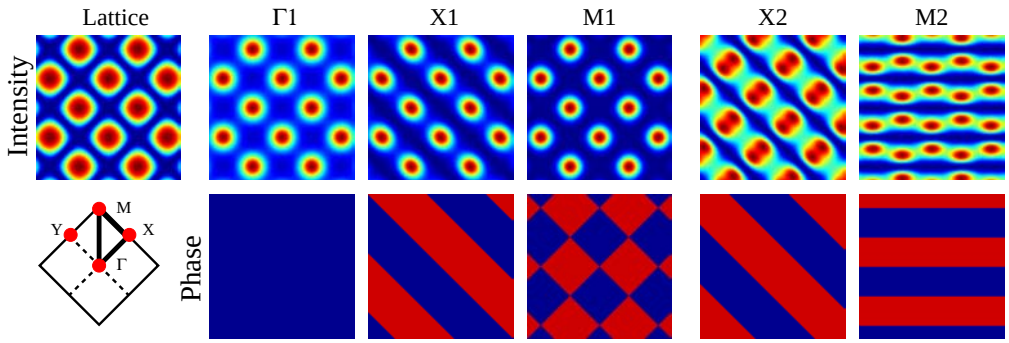

Fig. 2. Intensity (top) and phase (bottom) of different Bloch modes from the high symmetry points of the first and second band of a square lattice. The blue color for the phase distribution corresponds to the zero phase, while the red color corresponds to the π phase.

electro-optic coefficient and the applied DC electric field, lattice modulation is $I_g = 0.49$, and $d = 23\,\mu$m is the lattice period.

Such a periodic modulation of the refractive index results in the formation of a bandgap spectrum for the transverse components of the wave vectors K_x and K_y. Then the propagation of linear waves through the lattice is described by the spatially extended two-dimensional eigenmodes, known as the two-dimensional Bloch waves. They can be found as solutions of linearized equation (1) in the form

$$E(x,y;z) = \psi(x,y)\exp(i\beta z + iK_x x + iK_y y), \tag{3}$$

where $\psi(x,y)$ is a periodic function with the periodicity of the underlying lattice, and β is the propagation constant. For a square lattice shown in Fig. 1(a), the dispersion relation $\beta(K_x,K_y)$ is invariant with respect to the translations $K_{x,y} \to K_{x,y} \pm 2\pi/d$, and therefore is fully defined by its values in the first Brillouin zone [Fig. 1(b, inset)]. The dispersion relation $\beta(K_x,K_y)$ for this lattice is shown in Fig. 1(b) where the high-symmetry points of the lattice are marked by red dots.

It is important to note that, for the chosen lattice parameters, there exists a full two-dimensional band gap between the first and the second spectral band. The existence of a typical bandgap structure of the lattice with a complete two-dimensional gap and the highly nonlinear properties of the photorefractive crystal make the optically-induced photonic lattice a direct *analog of a two-dimensional nonlinear photonic crystal*. Therefore, our experiments offer an ideal test-bench for the similar phenomena with highly nonlinear and tunable two-dimensional photonic crystals that may be studied in the future with fabricated structures in nonlinear materials.

The intensity and phase structure of the calculated Bloch waves for the high symmetry points of the lattice from the first and second spectral bands are shown in Fig. 2. The upper row shows the Bloch-wave intensity profiles and the bottom row shows the corresponding phase structure. As a reference, the first column shows the light intensity of the lattice itself. For the two-dimensional Bloch waves from the first band, the intensity distribution of all modes is reflecting the structure of the square lattice, with the intensity maxima coinciding with those of the lattice. However, the phase structure differs substantially. As can be seen from Fig. 2, the phase of the two-dimensional Bloch waves originating from the Γ_1 point is constant. The phase structure becomes nontrivial for the modes from the X_1 and M_1 points. For the X_1 (Y_1) point, the phase represents a stripe-like pattern being constant along one principal direction of the lattice and exhibiting π phase jumps along the other direction. For the Bloch waves originating

#10229 - $15.00 USD Received 9 January 2006; received 15 February 2006; accepted 17 February 2006

from the M_1 point the phase distribution resembles a chessboard pattern.

On the other hand, the two-dimensional Bloch modes from the second spectral band have the intensity maxima centered between the maxima of the square lattice. The phase structure has a form of stripes oriented along one of the principal directions of the two-dimensional lattice for the X_2 point, or in 45° with respect to the principal axes for the M_2 point. The Γ_2 point appears to be nearly degenerate with the propagation constants nearly the same for the second, third, and fourth bands, and we do not consider it here.

The difference in the phase structure of the two-dimensional Bloch waves translates into the differences in propagation dynamics for beams of a finite size which spectrum is localized in the vicinity of the corresponding high-symmetry points in the Brillouin zone. Indeed, the alternating phase is a signature of strong Bragg scattering, that may lead to an enhanced diffraction of beams similar to the effect of the dispersion enhancement in the Bragg gratings [33]. Therefore, the beams can experience anisotropic diffraction due to the asymmetric phase structure of the corresponding Bloch waves, and this can be detected by analyzing the beam broadening in the linear regime.

The sign of the curvature of the related dispersion surface can be identified experimentally utilizing the nonlinear self-action of the beam. In the case of a medium with positive (self-focusing) nonlinearity, increasing input beam intensity will result in either focusing or defocusing of the output beam depending on whether the curvature of the dispersion surface is convex or concave, respectively. A close examination of the spatial dispersion defined by the bandgap spectrum of the lattice [Fig. 1(b)] shows that the beams associated with the Γ_1 and X_2 points will experience self-focusing in both (x,y) directions due to the convex curvature along the x and y directions. On the other hand, the beams associated with the M_1 point will experience nonlinear self-spreading due to the concave curvature at the corresponding point of the dispersion surface. Totally different behavior is expected for the beams associated with the X_1 point of the lattice spectrum, as the curvatures of the dispersion surface are opposite in the x and y directions. Such beams will experience an anisotropic nonlinear response: they will focus along the direction of the constant phase and at the same time will self-defocus in the orthogonal direction. The symmetry point M_2 of the dispersion curve is degenerate between the second and the third bands, with both bands having opposite but isotropic curvatures. Due to this degeneracy the nonlinear self-action of the beams associated with this point will result in a complex beam dynamics.

3. Experimental arrangements

In order to study experimentally the generation, formation and propagation of linear and nonlinear Bloch waves in two-dimensional photonic lattices, we implement the setup shown schematically in Fig. 3. An optical beam from a cw frequency doubled Nd:YVO_4 laser, at the wavelength of 532 nm, is split by a polarizing beam splitter into two beams with orthogonal polarizations. The vertically polarized beam is passed through a diffractive optical element (DOE), which produces two orthogonally oriented pairs of beams. An optical telescope combines these four beams at the input face of the photorefractive crystal, thus forming a two-dimensional square interference pattern which is stationary along the crystal length (see inset in Fig. 3). The period of this pattern is 23 μm. The crystal is a Cerium doped SBN:60 of 20 mm × 5 mm × 5 mm biased externally with a DC electric field of 4 kV/cm applied along the c-axis (horizontal). Due to a strong anisotropy of the electro-optic effect, the ordinary polarized lattice beams will propagate linearly inside the crystal, while in the same time inducing a refractive index modulation for the extraordinary polarized (probe) beam [32].

The second, extraordinary polarized laser beam is expanded by a telescope and illuminates the active area of a Hamamatsu programmable phase modulator (PPM). The modulated beam

#10229 - $15.00 USD Received 9 January 2006; received 15 February 2006; accepted 17 February 2006

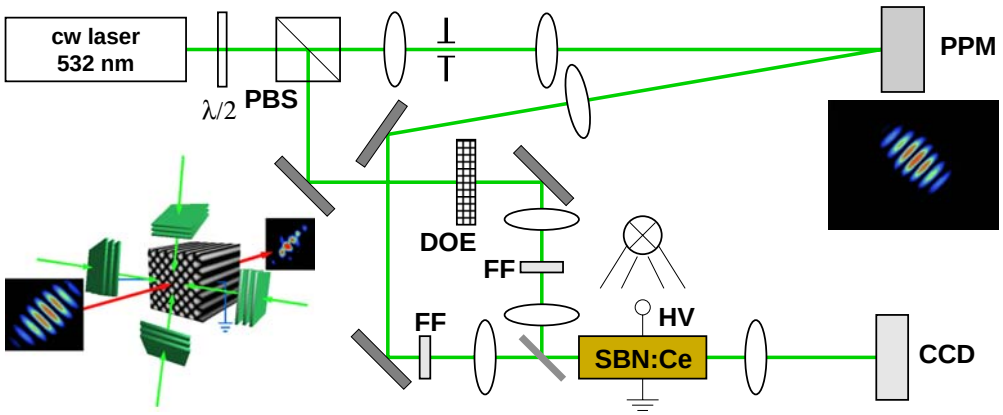

Fig. 3. Experimental setup for the excitation of two-dimensional Bloch modes: HV: High voltage, CCD: camera, FF: Fourier filter mask, $\lambda/2$: half wave plate; PPM: Programmable phase modulator, DOE: Diffractive optical element to produce four coherent beams, PBS: Polarizing beam splitter. Left inset: Geometry of the two-dimensional optical lattice. Right inset: Example of a phase and amplitude engineered wave in the optical lattice.

is then imaged by a large numerical aperture telescope at the input face of the photorefractive crystal. A spatial Fourier filter (FF) is placed in the focal plane of the telescope to eliminate higher-order spectral components and ensure that the optical beam entering the crystal will have the phase and amplitude structure required to match the specific Bloch mode. The modulated probe beam is combined with the lattice onto a beam splitter. Thus it will propagate onto the induced periodic index modulation and simultaneously will experience a strong nonlinear self-action at sub-micro-Watt range, due to the strong photorefractive nonlinearity. Both faces of the crystal can be imaged on a CCD camera by a high numerical aperture lens to capture beam intensity distribution.

In order to excite selectively different Bloch modes of the two-dimensional lattice, the optical beam must match their transverse amplitude structure. This is achieved by the use of PPM that converts the initially Gaussian probe beam into the desired amplitude and phase modulation at the front face of the photorefractive crystal. For low input intensity the incident probe beam, representing linear Bloch wave, does not affect the refractive index of the lattice and hence its propagation is completely determined by the dispersion at the particular point of the Brillouin zone. A finite beam will diffract with a rate depending on the value of the diffraction coefficients along the principal directions of the lattice. These diffraction coefficients are determined by the curvature of the dispersion surfaces along the x and/or y directions. With increasing power, nonlinear self-action of the beam will counteract its diffraction in the case of normal diffraction, but it will enhance the beam spreading in the case of the anomalous diffraction. These features of the nonlinear self-action of finite beams allows us to identify the character of the dispersion curves when the beam is associated with a specific Bloch mode of the lattice.

Our experiments are complemented by the numerical simulations of the underlying equation (1) with the initial conditions matching the transverse structure of the corresponding Bloch wave superimposed on a Gaussian carrier beam

$$E(x,y) = A\exp(-x^2/w_x^2 - y^2/w_y^2), \tag{4}$$

where A is a constant amplitude, w_x and w_y are the corresponding beam widths along the x and y axes, respectively. Our numerical simulations allow us to trace, with a high accuracy, the actual beam evolution inside the crystal that is not directly accessible in experiment, as well as

#10229 - $15.00 USD Received 9 January 2006; received 15 February 2006; accepted 17 February 2006

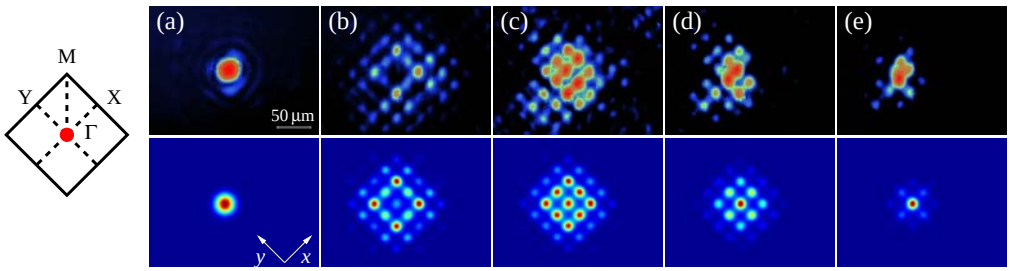

Fig. 4. Experimental data (top row) and numerical results (bottom) for the excitation of the two-dimensional Bloch waves from the Γ point of the first spectral band (Γ_1). (a) Input beam; (b-e) outputs for input powers of 25 nW, 125 nW, 250 nW, and 375 nW, respectively.

provide the opportunity to test the beam evolution for larger propagation distances beyond the experimentally accessible crystal lengths.

4. Excitation of the Bloch modes of the first band

First, we study experimentally the propagation of beams associated with different Bloch waves from the first spectral band of the lattice bandgap spectrum (Fig. 1).

4.1. Γ_1-point

The excitation of the point Γ_1 is realized simply by launching a Gaussian beam [Eq. (4)] along the lattice and having zero transverse wavevector components. The structure of this Bloch wave is fully symmetric along the principal axes of the lattice (Fig. 2). If the initial beam excites a single lattice site, then the diffraction output represents a typical discrete diffraction [34, 35] and it is well suited to characterizing the induced periodic potential. When the intensity of the initial beam is high enough, the nonlinearity induced index change leads to a shift of the propagation constant inside the total internal reflection gap [Fig. 1(b)] and gives rise to the formation of discrete lattice solitons [34, 35].

Our experimental results were performed with an input beam of width $w_x = w_y = 18\,\mu$m. For low input powers of 25 nW [see Fig. 4(a)] the beam undergoes strong discrete diffraction on the lattice, where most of its energy is transferred to the outside lobes. With increasing the laser power [Fig. 4(c-e)] the beam self-focuses leading to the formation of a discrete lattice soliton in agreement with previous experimental studies [34, 35]. The numerical simulations shown in Fig. 4 (bottom row) are in good agreement with the experimental observations.

4.2. X_1-point

The Bloch wave at the X symmetry point of the first band has a strongly asymmetric phase structure. This leads to anisotropic diffraction for the propagating beams associated with this Bloch mode, allowing for new types of waveguiding [36, 37] due to different curvatures of the dispersion surface in x and y directions. In order to balance the rate of beam broadening due to diffraction along these directions, in experiment the input beam is made elliptical, elongated in form of 3 humps along the x axis. Its phase is constant along the y direction and alternates by π along the perpendicular x direction [Fig. 5(a)] (The image is slightly overexposed, so outer lobes appear to be stronger than they are). This stripe-structure is launched on site, i.e. with position of the intensity maxima on lattice sites. In numerics, the input profile is modeled by the following expression

$$E(x,y) = A\cos(Kx)\exp(-x^2/w_x^2 - y^2/w_y^2),$$

#10229 - $15.00 USD Received 9 January 2006; received 15 February 2006; accepted 17 February 2006

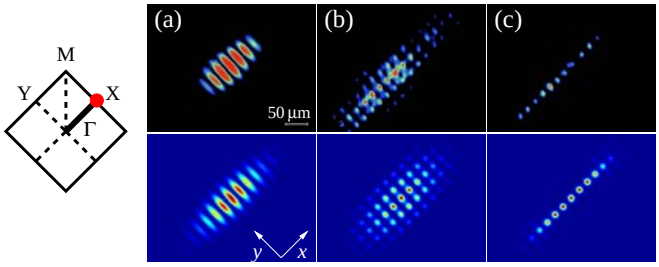

Fig. 5. Experimental data (top row) and numerical results (bottom) for the excitation of the two-dimensional Bloch waves from the X point of the first spectral band (X_1). (a) Input beam; (b,c) outputs for input powers of 25 nW and 375 nW, respectively.

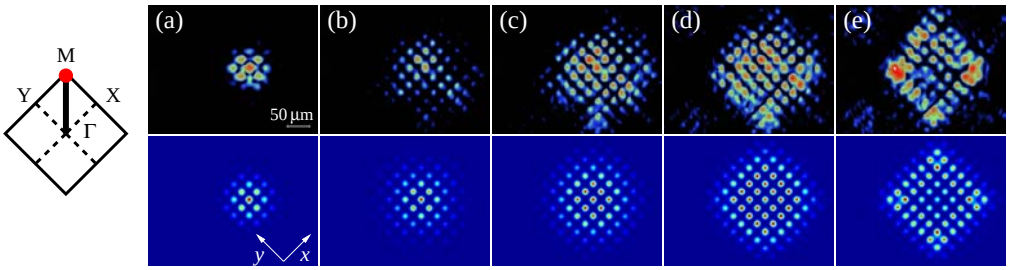

Fig. 6. Experimental data (top row) and numerical results (bottom) for the excitation of the two-dimensional Bloch waves from the M point of the first spectral band (M_1). (a) Input beam; (b-e) outputs for input powers of 40 nW, 125 nW, 300 nW, and 850 nW, respectively.

where $w_x = 100\,\mu$m, $w_y = 33\,\mu$m and $K = \pi/d$ is the lattice wavevector.

Our experimental results and the corresponding numerical simulations show the same behavior for the nonlinear response of the beam at the output face of the crystal [Fig. 5(b,c) top and bottom row respectively]. At low laser powers, the initial beam spreads strongly in x-direction due to the larger curvature of the dispersion surface. Increasing beam power leads to strong focusing of the beam along y direction and beam spreading along x axis. This difference in the nonlinear self-action of the beam allows one to identify experimentally that the dispersion surface has opposite curvatures in two principal directions of the lattice as follows from the theoretically calculated band-gap diagram [Fig. 1(b)]. The process of strong focusing along the non-modulated y direction is closely related the effect of grating mediated waveguiding [36, 37].

4.3. M_1-point

The structure of the dispersion surface near the M symmetry point of the first band is symmetric in x and y directions. To match the Bloch-wave profile, the input beam is modulated such that it represents humps of alternating phase in the form

$$E(x,y) = A\cos(Kx)\cos(Ky)\exp(-x^2/w_x^2 - y^2/w_y^2),$$

with $w_x = w_y = 51\,\mu$m [Fig. 6(a)].

The curvature of the dispersion surface is concave as indicated in Fig. 1(b). Therefore the initial beam is expected to exhibit enhanced defocusing with increasing of the beam power. Our experimental measurements of the output beam intensity distribution are depicted in Fig. 6. At low laser powers ($P = 40$ nW) the beam diffracts linearly forming a Bloch state from the M_1-

#10229 - $15.00 USD Received 9 January 2006; received 15 February 2006; accepted 17 February 2006

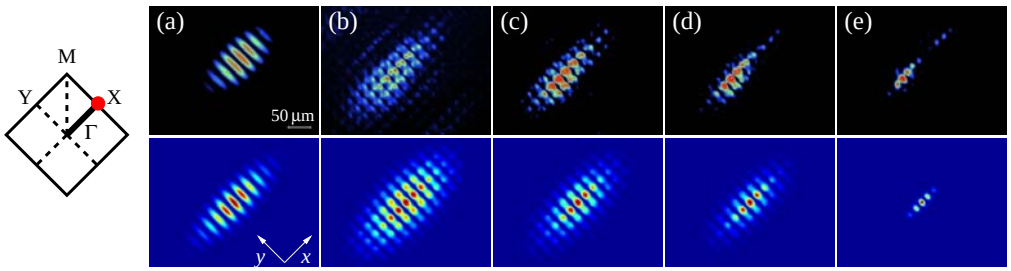

Fig. 7. Experimental data (top row) and numerical results (bottom) for the excitation of the two-dimensional Bloch waves from the X point of the second spectral band (X_2). (a) Input beam; (b-e) outputs for input powers of 20 nW, 50 nW, 100 nW, and 200 nW, respectively.

symmetry point, shown in Fig. 6(b). With increasing power [Fig. 6(c-e) at power levels 125 nW, 300 nW, and 850 nW, respectively] the beam defocuses as expected and forms a square type pattern [Fig. 6(e)]. Similar behavior is also observed in the performed numerical simulations [Fig. 6, bottom row].

5. Excitation of the Bloch modes of the second band

The second band of the lattice bandgap spectrum is separated from the first band by a two-dimensional photonic gap. The Bloch modes from the top of the second band (as the X symmetry point) then can be moved by nonlinearity inside the gap, leading to the formation of spatially localized gap solitons. On the other hand, the second band overlaps with the higher-order bands at the Γ and M points leading to degeneracy of the two-dimensional Bloch modes and subsequently complex beam dynamics that are reproducible in numerical simulations and experiments but difficult to interpret. Out of these degenerate points, below we consider only the M symmetry point.

5.1. X_2-point

In order to match the profile of the Bloch wave from the X symmetry point of the second band we use a modulated Gaussian beam, of the form

$$E(x,y) = A\cos[K(x-d/2)]\exp(-x^2/w_x^2 - y^2/w_y^2),$$

where the maxima of this modulated pattern [Fig. 7(a)] are shifted with respect to the lattice maxima by half a lattice period along the x axis. The structure of the dispersion surface of this Bloch mode is highly anisotropic, therefore the beam diffracts differently in x and y directions. To account for this anisotropic diffraction we used an elliptic beam elongated along the x axis with $w_x = 100\,\mu$m and $w_y = 33\,\mu$m. At low laser powers (20 nW) the beam diffracts linearly, while reproducing the structure of the Bloch wave from the X point of the second band (Fig. 2). With increase of the laser power [50 nW, 100 nW, and 200 nW for Fig. 7(c-e), respectively] the beam focuses in both transverse directions and forms a strongly localized state [Fig. 7(e)]. Such state represents the theoretically predicted gap solitons in photonic crystals [17, 18]. It has a reduced symmetry with respect to the lattice and it is formed by the combined action of Bragg reflection in x-direction and total internal reflection in y-direction [38]. The experimental data are in excellent agreement with the numerical simulations [Fig. 7(bottom row)].

We note that a symmetric superposition of X_2 and Y_2 states gives rise to symmetric gap solitons [17, 18] or gap vortices [39, 40].

#10229 - $15.00 USD Received 9 January 2006; received 15 February 2006; accepted 17 February 2006

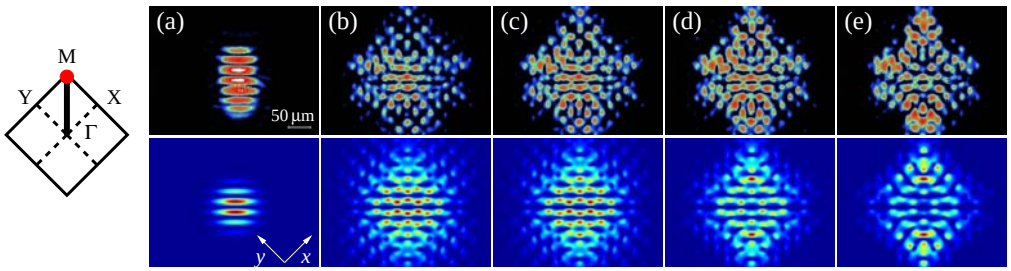

Fig. 8. Experimental data (top row) and numerical results (bottom) for the excitation of the two-dimensional Bloch waves from the M point of the second spectral band (M_2). (a) Input beam; (b-e) outputs for input powers of 25 nW, 90 nW, 270 nW, and 660 nW, respectively.

5.2. M_2-point

The M symmetry point of the second band is degenerate as the propagation constant coincides with that of the third band. Furthermore, two dispersion curves have opposite curvatures and therefore a complex beam dynamics is expected. We select the Bloch mode [Fig. 2] which structure can be approximated by horizontal stripes, that are oriented at a 45° angle with respect to the principal axes of the lattice. To match this Bloch mode we used a Gaussian beam modulated at 45° with respect to the x and y axes [Fig. 8(a)],

$$E(x,y) = A\cos(Kx+Ky)\exp(-x^2/w_x^2 - y^2/w_y^2),$$

with $w_x = w_y = 38\,\mu$m.

Linear propagation at low power is shown in Fig. 8(b), where the beam is strongly diffracting at the crystal output. At higher powers in (c) 90 nW, (d) 270 nW and (e) 660 nW the nonlinear self-action leads to strong beam reshaping. The central part of the beam experiences self-defocusing while the intensity in the outer region increases. Again, our experimental results are in good agreement with the numerical simulations [Fig. 8, bottom row].

6. Conclusions

We have generated experimentally and analyzed theoretically different types of two-dimensional Bloch waves of a square photonic lattice by employing the phase imprinting technique. We have excited selectively the Bloch waves belonging to different high-symmetry points of the two-dimensional photonic lattice, and demonstrated the unique linear and nonlinear anisotropic properties of the lattice dispersion resulting from the different curvatures of the dispersion surfaces of the first and second spectral bands. We have employed strong self-focusing nonlinearity of biased photorefractive crystals to study, for the first time to our knowledge, nonlinear self-action effects for the two-dimensional Bloch waves at the high-symmetry points of both fundamental and higher-order spectral bands. We have demonstrated that our experimental results are in an excellent agreement with the numerical simulations of both linear and nonlinear effects of the light propagation.

Acknowledgments

The authors acknowledge a support of the Australian Research Council, and thank Mark Saffman for providing a photorefractive crystal. D.T. thanks Nonlinear Physics Centre of the Research School of Physical Sciences and Engineering for a warm hospitality during his stay in Canberra, and also acknowledges grant and a travel support from Konrad-Adenauer-Stiftung e.V.

#10229 - $15.00 USD Received 9 January 2006; received 15 February 2006; accepted 17 February 2006